Journal of Engineering Science and Technology
Vol. 14, No. 4 (2019) 2292 - 2319

PLANNING OF BASE STATION AND RELAY STATION DEPLOYMENT LOCATIONS FOR NEXT GENERATION NETWORKS

VINOTH BABU KUMARAVELU[1,*], ARTHI MURUGADASS[2]

[1]School of Electronics Engineering, Vellore Institute of Technology,
Vellore Campus, Vellore, 632 014, Tamil Nadu, India
[2]Department of Computer Science and Engineering,
Sreenivasa Institute of Technology and Management Studies,
Chittoor, 517 127, Andhra Pradesh, India
*Corresponding Author: vinothbab@gmail.com

Abstract

The deployment of an adequate number of Relay Stations (RS) at proper sites will improve the network connectivity and energy consumption, which are the major requirements of next-generation networks. In this paper, an efficient four-stage uniform clustering scheme is proposed, which identifies the sites for Base Station (BS) and RS deployment from the available candidate sites. This paper considers uniform clustering based deployment as the base and tries to improve its performance by addressing the solutions to its pitfalls. Uniform clustering based deployment and throughput oriented path selection schemes are combined in this work, which maximizes the reach to destination without compromising the Quality of Service (QoS) even under link overloading conditions. The simulations are repeated for various network dimensions and the results show that the proposed scheme offers improved throughput and coverage ratio performances over the traditional Joint BS and RS placement (JBRP), Adaptive Cost based RS Deployment (ACRD), uniform clustering and fuzzy logic based schemes even under link overloading conditions without demanding additional cost.

Keywords: BS and RS deployment, Coverage ratio, Deployment budget, Link traffic overloading, Path selection, Throughput.

1. Introduction

In recent years, the requirement of multi-hop communication is growing rapidly [1]. The conventional telecom operators may prefer multi-hop deployment to expand their coverage area without spending too much cost for deployment and maintenance. The natural disasters and emergency situations cause lack of sufficient communication resources to cover the required geographic area [2]. It has been suggested to use multi-hop communication to extend the coverage to these areas. Due to its advantages, various standardization bodies like IEEE 802.11s [3], IEEE 802.16j [4], Long Term Evolution (LTE) [5-7], IEEE 802.11 ah [8] and Terrestrial Trunked Radio (TETRA) [9] have included multi-hop communication in their releases.

The concept of relaying is very popular in Vehicular Adhoc Networks (VANET), healthcare and Wireless Underground Sensor Networks (WUSN). VANETs are very popular for road safety measures and infotainment services [10]. The intermediate vehicles act as RSs to forward the messages to the sink node like Road Side Unit (RSU). Lai et al. [11] discussed the importance of RSs in healthcare. The observed abnormal variation of heart rate is communicated to remote care server through multi-hop communication by wireless in-home psychological monitoring system. It is very difficult to recharge buried sensor nodes in WUSNs. Power consumption is the primary objective of WUSN [12]. To improve the network lifetime, RSs are deployed above the ground to relay the traffic. The Macro and Pico serving nodes operate in same frequency band leading to interference. The interference degrades the channel quality. This leads to the low-rate transmission and wireless connection loss. To minimize interference, relay-assisted communication is proposed for the Internet of Things (IoT) [13].

In recent years, the investigation on the green cellular network has drawn great attention. It was measured that 2% of global CO_2 emissions are from Information and Communication Technology (ICT) industries [14, 15]. BSs consume 60%-80% of the total energy consumption of wireless networks [16, 17]. In Multi-Hop Relay (MHR) network, RSs are introduced between BS and Mobile Station (MS). This reduces the transmission distance and maximizes the throughput [18-20]. The concept of RSs are very popular in third generation partnership project (3GPP) LTE Rel-10 and beyond [21, 22]. The present research community discusses the role of relaying for 5G development [23-26].

The wireless links are more prone to channel variations. Due to the additional aspects like propagation losses and interference, connectivity becomes a more critical problem in wireless communication. Hence, providing robust network connectivity is a more challenging task [27]. The network connectivity is a function of channel conditions, node locations and protocol. Without altering the protocol and channel conditions, the network connectivity can be improved by the deployment of RSs. Kocan et al. [8] discussed the necessity of multi-hop communication in IEEE 802.11 [8]. It has been shown that the introduction of RSs is necessary to achieve the minimum required data rate of 100 kbps and the coverage distance of 1 km. The appropriate deployment of RSs is the most feasible solution to repair the network topology [28]. The deployment of adequate number of RSs at proper sites results in higher energy consumption.

Lu and Liao [29] proposed a two-stage Joint BS and RS Placement (JBRP) scheme to maximize the network capacity. The algorithms are developed based on

coverage and deployment cost constraints. Even though JBRP scheme addressed the budget and coverage constraints, it suffers from imperfect load distributions. Imbalance in traffic load will lead to a larger packet queuing delay and loss in system throughput. This is a severe issue from the customer point of view. The unsatisfied customer will move to the competitive operator. It is also assumed that the candidate sites of RSs are same as the locations of Demand Nodes (DN) [30] and the candidate sites of BSs are assumed to be the corner of DNs. This is an impractical and unreasonable assumption.

Aguero et al. [1] discussed the benefits of multi-hop communication over traditional single-hop communication. In this work, two different access point (AP) deployment strategies are analysed. First one is random deployment, where no prior network planning is considered. This resulted in poor connectivity. The second one is array deployment, which maximizes the coverage over random deployment. Aguero et al. [1] also developed analytical expressions for the probability of a customer to be disconnected from an AP. However, the authors presumed that the APs are deployed without having the knowledge of global network topology.

Zhang et al. [31] proposed a distance-aware RS deployment algorithm for worldwide interoperability for microwave access (WiMAX) mesh networks. The authors presented two approximation algorithms to effectively deploy a minimum number of RSs to meet the customer requirements in terms of signal quality and data rate. Wu and Feng [32] proposed an energy efficient RS deployment scheme, which introduces an appropriate number of RSs into the cellular network at proper sites to improve energy efficiency without compromising the throughput.

Chang and Chen [33] proposed to address the trade-off among the deployment cost, coverage and throughput, a uniform clustering based BS and RS deployment scheme. This algorithm provides reasonable throughput and coverage by balancing the network throughput between different BSs.

Chang et al. [34] proposed an Adaptive Cost based RS Deployment (ACRD) scheme by considering five different quality factors like transmission quality, deployment cost, service coverage with and without population and RS overlapping index. Then a cost function is modelled in terms of all the above-mentioned quality factors. The optimization problem is solved for the least network cost. This approach also considers the deployment of three different types of RS namely fixed, nomadic and mobile. The simulation results demonstrate that ACRD scheme maximizes the transmission quality, service coverage and minimizes the system cost, inter-RS interference than the Random Deployment (RAND), Static Average Weighting (SWA) and Dynamic Average Weighting (DWA) approach. It is also shown that the ACRD approach deploys the number of RSs on the high-density populated areas than the other areas. However, this scheme is tested for a small 2 km × 2 km geographic area with a smaller number of MSs. This scheme also assumes a maximum number of RS deployment combinations. The computational complexity of this scheme increases with the number of RS deployment combinations.

Chang and Lin [35] proposed the fuzzy logic based BS and RS placement approach, where the coverage ratio and Traffic Ratio (TR) of each candidate sites are given as the input for Fuzzy Inference Engine (FIE). The Selection Factor (SF) corresponding to each candidate site is the output from the FIE. The authors have framed Mamdani triangular membership functions for coverage ratio, TR and SF.

Based on two input parameters, they have framed nine rules. The proposed approach chooses the candidate sites with highest SF based on the coverage and budget constraints. Even though the uniform clustering and fuzzy logic based schemes perform better than JBRP scheme, it suffers by a number of issues. Here, by considering coverage and budget constraints, two separate algorithms are proposed. Based on the requirement, BS has to select one between these two algorithms. The effectiveness of BS in enabling proper switching between these two algorithms is not discussed in the current works. The capacity of the RS is limited when compared to the BS. When there exists a non-uniform traffic demand from an RS, the problem of link overloading arises [36]. Link overloading leads to disappointing network throughput. The effect of link overloading on the proposed BS and RS deployment schemes are not discussed in the current works. Similarly, co-channel interference, which is a severe issue in MHR networks, is also not considered. The simulation results show that the average throughput for the proposed scheme is less than the conventional throughput based BS and RS deployment schemes. Similarly, the coverage ratio of the proposed scheme is less than the conventional coverage based BS and RS deployment schemes. There are no special considerations in the current works for improving network throughput.

Chen et al. [16] proposed an extended Hungarian algorithm based energy efficient mobile RS deployment scheme, which selects the deployment sites from the available candidate sites. This scheme maximizes energy efficiency while guaranteeing the spectral efficiency and coverage requirements. This algorithm is based on minimum movement distance and it outperforms greedy and static deployment algorithms. Li et al. [37] proposed an algorithm to identify optimal sites for RS deployment, which maximizes the reach to destination without compromising the QoS requirements. Liao et al. [38] addressed the necessity of mobile RSs in multi-hop communication. The mobile devices may move in and out of the fixed RS's coverage area. This leads to unessential handovers, which causes a low data rate and load imbalance. Liao et al. [38] proposed to minimize these issues, minimum mobile RS path selection algorithm to deploy the required number of mobile RSs in the given geographic area. Mobile RSs can be deployed in systems like public transportation to reduce the deployment cost and to serve mobile users.

Various network performance metrics like throughput, coverage and lifetime can be considered as the goals for the deployment of RSs. Magan-Carrion et al. [39] proposed to maximize network connectivity, a new RS deployment scheme. According to Cheng et al. [27], the convex optimization problem is formulated to identify the precise candidate sites for RS deployment, which improves the network connectivity. Path selection is one of the critical issues in MHR networks [40]. Wang et al. [40] proposed a path selection scheme is proposed based on the Radio Resource Utilization Index (RRUI). However, this algorithm fails under link overloading conditions. Wang et al. [36] proposed a Load-Aware Spectral Efficient Routing (LASER) based path selection scheme, which uses link spectral efficiency as the metric for path selection. This algorithm is proved to be better performing under link overloading conditions. Thus, in the proposed work, the authors adopt a LASER based path selection to address the link overloading issue.

Placing an RS in a well-covered area is meaningless. The proposed work encourages deploying RSs on the cell edges with sufficiently far distance to avoid co-channel interference. To maximize the coverage and the throughput by keeping the deployment cost low, the algorithm also encourages deploying more number of RSs

than the BSs. By including all the mentioned factors, our new algorithm has been developed and it offers better coverage and throughput performance than the conventional JBRP, ACRD, uniform clustering and fuzzy logic based schemes. Our proposed modified uniform clustering based BS and RS deployment scheme has the competency to present the network operator a competent BS and RS deployment scheme for next-generation networks.

The rest of the manuscript is planned in the following way: Section 2 introduces the system model and Section 3 introduces the proposed BS and RS deployment scheme. Section 4 discusses the simulation results and Section 5 concludes the paper by highlighting the future works.

2. System Model

We consider a geographic area where the BSs and RSs have to be deployed to offer the services to the customers. It is assumed that a large number of MSs is randomly located across the area with non-uniform traffic demands. The deployed BSs are directly connected to the core network through the wired backhaul connection. BSs are responsible for data transmission between BS and MS. It also acts as a deciding authority for path selection when there exist multiple paths between BS and MS. The deployed RSs do not have a direct backhaul connection to the core networks [21]. RSs are usually mounted on the towers or top of the buildings. The functionalities and cost of the RSs are much lower than the BSs. The comparisons between macro BS and RS are listed in Table 1. The deployment of BS and RS should be efficient in such a way that each MS within the geographic area must have a connection at least with a BS or an RS. All the BSs are connected to Mobile Switching Centre (MSC), which acts as a gateway between the existing wired and wireless networks. The MHR network model is illustrated in Fig. 1.

Table 1. Comparison between MHR BS and RS [20].

Parameters	BS	RS
Transmission power (W)	20-40	2-20
Cell radius (km)	≥ 3	1.9
Bandwidth (MHz)	100	50
Location	Outdoor	Outdoor/Indoor
Installation	Operator	Operator
Cost (Euros)	397800	55692
Capacity (MSs)	> 256	32-120

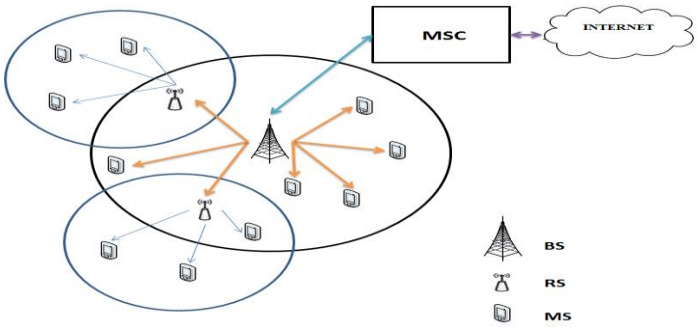

Fig. 1. LTE-A MHR network.

Since we mainly focus on cell edge users, the deployment of transparent RSs is not considered in this work. We assume a simple free space propagation model for path loss measurements. However, this work can be extended to transparent RS by considering the effect of shadowing and multipath. Chang and Chen [33] given as per the free space model, the Signal to Noise Ratio (SNR) of a link.

$$SNR(dB) = 10 log_{10}\left(\frac{P_r}{\sigma_n^2}\right) \tag{1}$$

where σ_n^2 is the noise variance and P_r is the received signal power, which is given by as follows:

$$P_r = P_t\left(\frac{c}{4\pi fd}\right)^2 \tag{2}$$

where P_t is the transmitted signal power, f is the carrier frequency, c is the velocity of light and d is the distance between any two communicating stations. To increase the data transmission rate and to minimize the Bit Error Rate (BER), the proposed system uses different Modulation and Coding Schemes (MCS). BS offers flexible modulation and coding schemes to each user based on their channel conditions.

The MCS used in this work is listed in Table 2. From Table 2, it is clear that the lower burst profiles offer less data rate and higher burst profiles offer a high data rate. Based on the distance between the communicating nodes, the BS offers a burst profile for each link [33, 41]. The ultimate aim of introducing RS is to decrease the distance between the communicating nodes and to use the higher burst profiles [35]. LTE-A and IEEE 802.16 j standards use Binary Phase Shift Keying (BPSK), Quadrature Phase Shift Keying (QPSK) and quadrature amplitude modulation (QAM) schemes to support different rates to different users.

The deployment problem can be formulated as follows:

Define the BS and RS candidate position vectors.

$$B^c = [1,2 \ldots b] \tag{3}$$

$$R^c = [1,2 \ldots r] \tag{4}$$

where b and r represents the number of candidate positions of BS and RS respectively.

Table 2. MCS scheme for link adaptation [41].

Burst profile	Coding rate	Modulation	Distance between nodes (km)	SNR (dB)	Data rate (Mbps)
1	1/2	BPSK	3.20	3.00	1.269
2	1/2	QPSK	2.70	6.00	2.538
3	3/4	QPSK	2.50	8.50	3.816
4	1/2	16-QAM	1.90	11.50	5.085
5	3/4	16-QAM	1.70	15.00	7.623
6	2/3	64-QAM	1.30	19.00	10.161

7	3/4	64-QAM	1.20	21.00	11.439

The objective of the algorithm is to maximize the average throughput per user, which is given by:

$$\overline{V} = \frac{\left(\sum_{i=1}^{M} R_i^{MS} . \alpha_i\right)}{\left(\sum_{i=1}^{M} \alpha_i\right)} \tag{5}$$

where R_i^{MS} is the transmission rate between BS and i^{th} MS, M is the total number of MSs in the geographic area and α_i is the binary function, which is given by,

$$\alpha_i = \begin{cases} 1 & ;if\ i^{th}\ MS\ is\ connected\ with\ any\ BS\ or\ RS \\ 0 & ;else \end{cases} \tag{6}$$

Subjected to:

- The co-channel interference constraint is given by:

$$d(RS(i), RS(j)) > d_I \quad , i \neq j \tag{7}$$

where $d(RS(i), RS(j))$ is the distance between two RSs, $RS(i)$ and $RS(j)$ and d_I is the interference threshold distance.

- The deployment budget constraint is given by,

$$\sum_{i=1}^{b} C_i^{BS} . \beta_i + \sum_{i=1}^{r} C_i^{RS} . \gamma_i \leq T \tag{8}$$

where C_i^{BS} and C_i^{RS} are the deployment cost of i^{th} BS and RS respectively. T is the total deployment budget, β_i and γ_i are binary variables, which are given by,

$$\beta_i = \begin{cases} 1 & ;if\ BS\ is\ deployed\ in\ candidate\ position\ i \\ 0 & ;else \end{cases} \tag{9}$$

$$\gamma_i = \begin{cases} 1 & ;if\ RS\ is\ deployed\ in\ candidate\ position\ i \\ 0 & ;else \end{cases} \tag{10}$$

- The coverage ratio obtained should be greater than the expected coverage (ECR)

$$CR \geq ECR \tag{11}$$

The two-phase transmission nature of the MHR network may reduce the capacity and lead to unnecessary delay in transmission. The BS has to decide for an indirect transmission, only when it is needed. This problem is severe when the MSs are connected by both BS and RS. Since the motive is to maximize the network throughput and to reduce the delay, the BS uses throughput oriented selection rule to decide about direct or indirect communication. The indirect transmission is preferred as long as [14]

$$R_{brm} > R_{bm} \tag{12}$$

where R_{brm} is the data transmission rate between BS, RS and MS and R_{bm} is the data transmission rate between BS and MS.

The data transmission rate of indirect transmission is given by,

$$R_{brm} = \frac{P}{t_{BS-RS-MS}} = \frac{P}{\frac{P}{R_{br}} + \frac{P}{R_{rm}}} = \left(\frac{1}{R_{br}} + \frac{1}{R_{rm}} \right)^{-1} \tag{13}$$

where P is the packet size, $t_{BS-RS-MS}$ is the transmission time from BS to MS through RS. R_{br} is data transmission rate of the link between BS and RS and R_{rm} is data transmission rate of the link between RS and MS.

Based on the throughput-oriented scheme, the data transmission rate of a user is as follows:

$$R = Max\left(R_{brm}, R_{bm}\right) \tag{14}$$

There exists a drawback in the throughput-oriented scheme. Based on (12), there are chances that multiple MSs may choose the same RS. As mentioned earlier, the functionalities and the capacity of the RS is limited when compared to the BS. This may lead to a severe issue called link overloading [36]. This issue may cause a severe quality loss in terms of throughput and packet queuing delay. It has been proved that the LASER based path selection scheme offers better throughput performance over link traffic overloading conditions. When the traffic demand from a particular RS exceeds its maximum capacity, the BS has to handover the services of few MSs to the neighbouring RSs from the link overloaded RS. In case of no neighbouring RS or link overloaded neighbouring RSs, the BS has to prefer for direct connection. The concept of link traffic overloading is illustrated in Fig. 2.

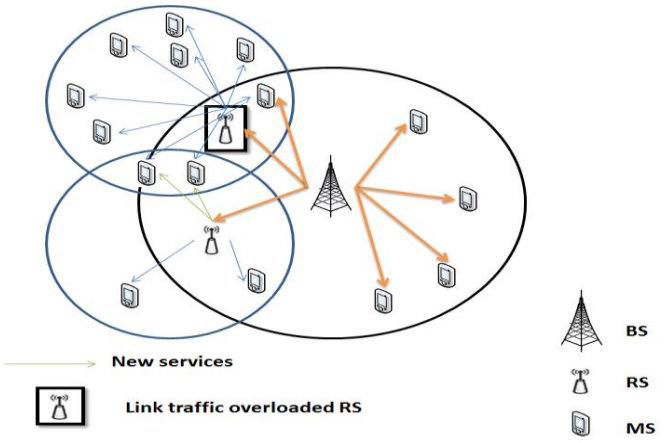

Fig. 2. Concept of link traffic overloading in MHR network.

The data rate of each link is calculated using Table 2. For every MS, the net transmission rates for all its possible downlink paths are calculated. Wang et al. [36] given the total transmission rate of l^{th} path of i^{th} MS.

$$R^{l}(i) = \sum_{k=0}^{L^{l}(i)-1} R^{l}_{k,k+1}(i) \quad ,l = 1,...N_{p}(i) \tag{15}$$

where l is the path index, i is the MS index, k is the node index, $N_p(i)$ is the number of possible downlink paths of a i^{th} MS and $L^{l}(i)$ is the length of the l^{th} path of a i^{th} MS. The BS has to select the path with the highest transmission rate. When there is a link traffic overloading, the BS has to choose the next highest transmission rate path.

3. Proposed BS and RS deployment scheme

The flow diagram of the 4-stage modified uniform clustering scheme is shown in Fig. 3. The flow diagram of the cluster formation stage is shown in Fig. 4. The performance of the uniform clustering based BS and RS deployment scheme is poor under link traffic overloading conditions. To maximize the network throughput even under link traffic overloading conditions, the proposed scheme combines uniform clustering based deployment, throughput oriented selection rule and LASER based path selection schemes. The proposed algorithm also tries to minimize the usage of indirect transmission as much as possible to reduce the transmission delay.

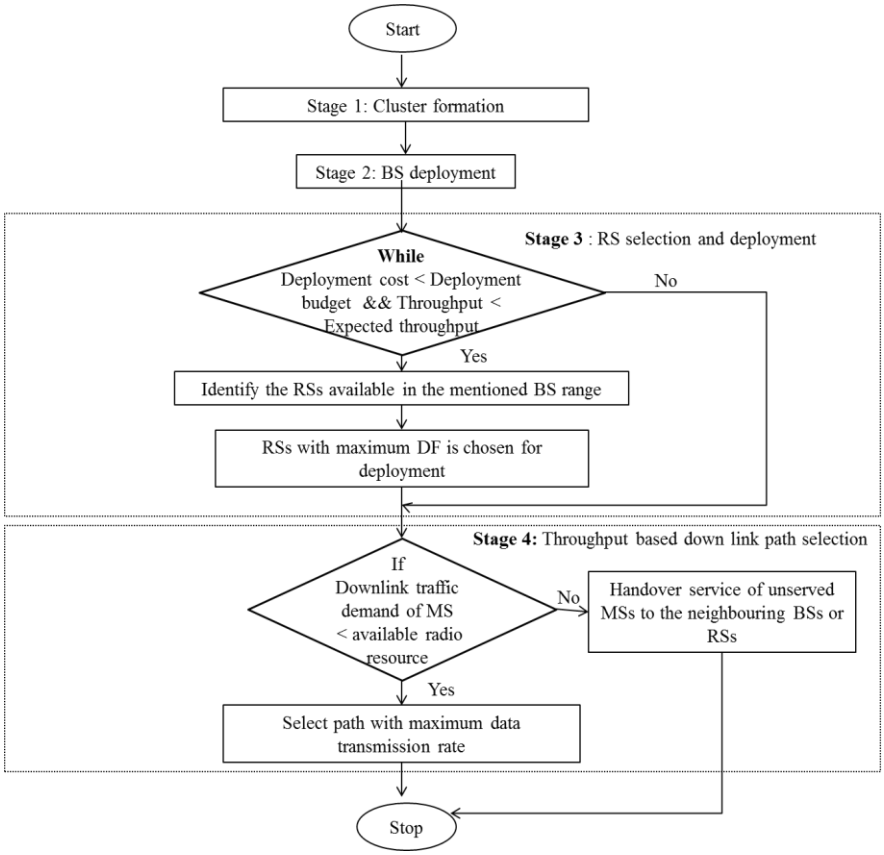

Fig. 3. Flow diagram of 4-stage modified uniform clustering scheme.

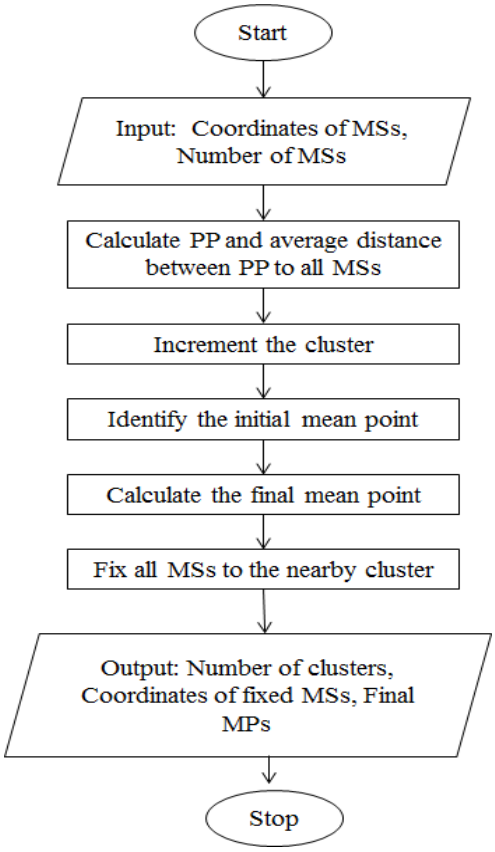

Fig. 4. Flow diagram of cluster formation stage.

The proposed scheme is executed in four stages. In stage 1, the clusters are formed based on the locations of the MSs, which is explained in Fig. 5. The coordinates of MSs (Z_i) and the total number of MSs in the geographic area are given as the input for stage 1. The number of clusters formed (s), the number of MSs joined to the j^{th} cluster (U_j) and the coordinates of the final mean point (MP) are the output from this stage.

The number of clusters formed is initialized to zero. In step 1, the Pivot Point (PP) is identified based on the coordinates of MSs. In step 2, the average Distance (D) between PP to all the MSs in the geographic area is calculated. The number of clusters formed is incremented by one in step 3.

The coordinates of the initial MP (m_{jx} , m_{jy}) of each cluster are identified between steps 4 to 7. In step 10, the distances between every MS to all the MPs are identified. In step 12, each MS is assigned to a cluster (C) with minimum distance. The new MP is identified for every cluster based on the coordinates of MSs connected to every cluster.

This is done in step 15 using (20). The steps 8 to 16 are repeated until all the MSs are fixed to a particular cluster. The PP and MP identification are illustrated in Fig. 6.

Stage 1: Cluster formation

Input: Z_i, M

Output: s, U_j, MP

Initialization: $s=0$

1. Identify the PP using

$$PP = \frac{1}{M}\sum_{i=1}^{M} Z_i \tag{16}$$

2. Calculate the average distance between PP to all the MSs in the geographic area using $D = \frac{1}{M}\sum_{i=1}^{M}|Z_i - PP|$ (17)

3. $s=s+1$
4. for $j=1$ to s
5. $m_{jx} = D\cos\left(\frac{2\pi}{s}(j+1)\right) + PP_x$ (18)
6. $m_{jy} = D\sin\left(\frac{2\pi}{s}(j+1)\right) + PP_y$ (19)
7. **end for**
8. **for** $i=1$ to M
9. **for** $j=1$ to s
10. $e(j) = |MP(j) - Z_i|$
11. **end for**
12. Find j corresponding to min $\boldsymbol{e}$ then $Z_i \in C_j$
13. **end for**
14. **for** $j=1$ to s
15. $MP(j) = \frac{1}{U_j}\sum_{i=1}^{U_j} Z_i(j)$ (20)
16. **end for**
17. Iterate steps 8 to 16 until each MS is fixed to a cluster

Fig. 5. Cluster formation stage.

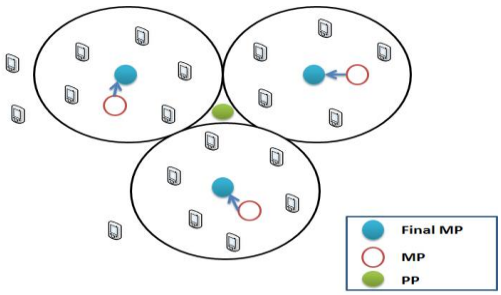

Fig. 6. Process of final MP calculation.

The flow diagram and algorithm for BS deployment based on the clusters formed in stage 1 is illustrated in Figs. 7 and 8 respectively. The candidate locations of BS, the number cluster formed, the coordinates of MSs joined to j^{th} cluster ($\boldsymbol{U_j}$)

and the final MP are the inputs for the stage 2. The selected BS locations (*SBS*), the total deployment cost (T_c), average throughput obtained ($\overline{V}$) and Coverage Ratio (CR) are the outputs from this stage. The average throughput and deployment cost are initialized to zero. *SBS* is initialized to null. The distance between every candidate locations of BS to every final MP is identified in step 3. In step 5, the BS candidate location nearer to the final MP is chosen for deployment. One BS location is selected for every cluster. After each BS selection, the T_c value is updated in step 6. This process is iterated between steps 1 to 7 for all the selected clusters. In step 8, *CR* is obtained using the number of covered MSs (M_{CMS}). In step 9, the average throughput per user is obtained using (5).

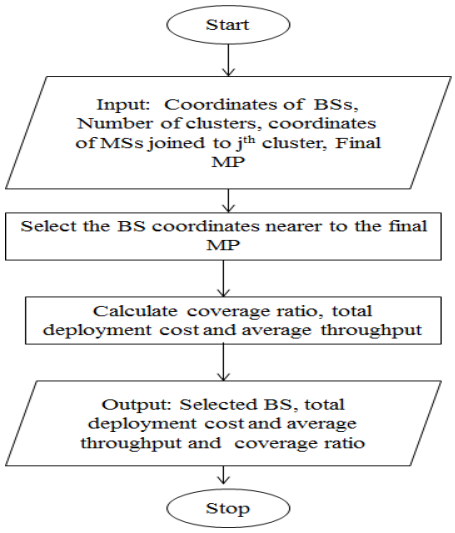

Fig. 7. Flow diagram of BS deployment stage.

Stage 2:BS deployment

Input: B^c, s, $\boldsymbol{U_j}$, MP

Output: ***SBS***, T_c, $\overline{V}$, CR

Initialization: $\overline{V}=0$, $T_c=0$, SBS=null

1. for j=1 to s
2. **for** m=1 to b
3. $e(m)=\left|B^c(m)-MP(j)\right|$
4. **end** for
5. Find m corresponding to min e then
   $SBS(j)\leftarrow B^c(m)$
6. $T_c=T_c+C^{BS}$ (21)
7. **end for**
8. $CR=\frac{M_{CMS}}{M}$ (22)
9. Obtain average throughput per user using (5)

Fig. 8. BS deployment stage.

The flow diagram and algorithm for RS selection and deployment is illustrated in Figs. 9 and 10 respectively. The selected BS, candidate locations of RS, the radius of BS $\left(R_{BS}\right)$, total allocated deployment budget, expected average throughput $\left(\overline{V_E}\right)$, total deployment cost and average throughput obtained from the previous stage are given as the input for this stage. The selected RS for deployment (*SRS*), updated T_c, $\overline{V}$ and *CR* is the output from this stage. In step 2, the conditions for total deployment cost and average throughput are checked. If the conditions are not met, then the RSs are deployed. To increase the coverage and to maximize the throughput of the cell edge users, the RS in the cell edge are given high priority. In step 4, the RS candidate locations available between $(2/3)R_{BS}$ and R_{BS} radius range are identified. The availability of RS candidate locations in the above said the range is verified in step 6. This idea is illustrated in Fig. 11. If the number of RS candidate locations (r^j) in the above said the range is not null, then Deployment Factor (*DF*) for every RS candidate location in the mentioned range is identified in step 8. The DF of n^{th} RS candidate location is calculated based on the average distance from all the uncovered MSs to n^{th} RS location ($d_{RS,\,n}$), a number of uncovered MSs (M_{UMS}) and the total traffic demands of uncovered MSs ($U_{RS,\,n}$).

The RS candidate location with maximum DF is identified in step 11. In step 12, the identified RS candidate location is stored in SRS and the corresponding *DF* is made to zero in step 13. The total deployment cost is updated in step 14. All these steps are repeated for all the identified clusters. If the conditions in step 19 are met, then the RSs are deployed in the selected RS candidate locations. Otherwise, go to step 3 in stage 1 so that new BS clusters can be formed to meet the required objectives. The coverage ratio and average throughput per user are updated in step 24.

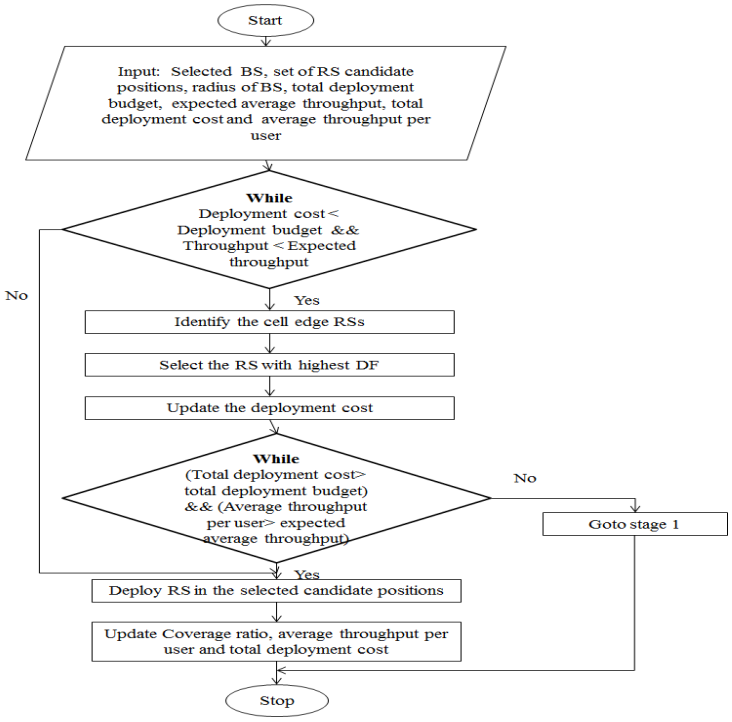

Fig. 9. Flow diagram of RS selection and deployment stage.

Stage 3: RS selection and deployment

Input: ***SBS,*** R^c, R_{BS}, T, $\overline{V_E}$,T_c, $\overline{V}$

Output: ***SRS***, T_c, $\overline{V}$, CR

Initialization: ***SRS***=null

1. **for** j=1 to s
2. **while** $\left(\left(T_c < T\right) \&\& \left(\overline{V} < \overline{V_E}\right)\right)$ do
3. **for** n=1 to r
4. Find $R^c(n)$, i.e the coordinates of RSs falls within the range [***SBS****(j)* + $\frac{2}{3}R_{BS}$, ***SBS****(j)*+ R_{BS}] of j^{th} BS
5. **end for**
6. **if** r^j!=null
7. **for** n=1 to r^j
8. $$DF(n) = \frac{1}{d_{RS,n}}\left(M_{UMS}\right)\left(U_{RS,n}\right) \quad (23)$$
9. **end for**
10. **for** n=1 to r^j
11. [value index]=Max(***DF***)
12. $SRS(n) \leftarrow R^c(index)$
13. ***DF***(index)=0
14. $T_c = T_c + C^{RS}$
15. **end for**
16. **end if**
17. **end while**
18. **end for**
19. **if** $\left(\left(T_c > T\right) \&\& \left(\overline{V} > \overline{V_E}\right)\right)$
20. Deploy the RSs in the selected candidate positions
21. **Else**
22. Go to step 3 in stage 1, (i.e) cluster formation stage
23. **end if**
24. Update CR and $\overline{V}$

Fig. 10. RS selection and deployment stage.

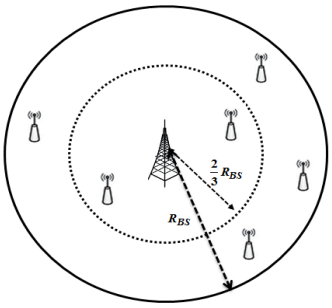

Fig. 11. Concept of cell edge RS selection.

In the fourth stage, throughput based downlink path selection is carried out for every covered MS. The process of path selection for every covered MS is carried out by the BS. The major steps involved in path selection are outlined in Figs. 12 and 13. The number of possible downlink paths of every covered MS is the input for this stage. The downlink path identified for every MS is the output from this stage. Before path selection, the resource availability check is carried out in step 2. The new service requesting MS will be served only when there is sufficient bandwidth and power resources. The unserved MSs are handed over to the neighbouring BS or RS based on the existence of radio resources. The data transmission rate of every MS through different downlink paths are determined using (15) in step 7. BS chooses a path, which can offer maximum throughput. This process is repeated for all the covered MSs in the geographical area.

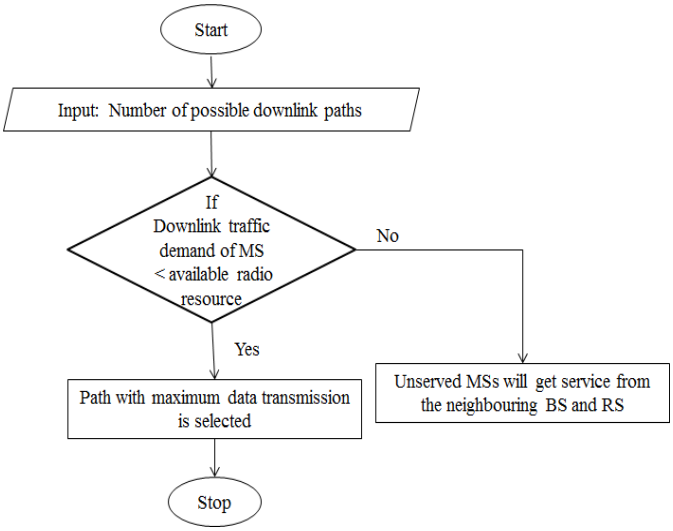

Fig. 12. Flow diagram of throughput based down link path selection stage.

Stage 4: Throughput based downlink path selection for MSs
Input: Number of possible downlink paths for every MS (N_p)
Output: Maximum throughput path selected for every MS (P^l)
1. **for** i=1 to M_{CMS} 2. **if** the downlink traffic demand of *MS(i)* is less than the available radio resources of BS **then** 3. **for** l=1 to $N_p(i)$ 4. **for** k=0 to $L^l(i)-1$ 5. Calculate $R^l_{k,k+1}(i)$ 6. **end for** 7. Calculate $R^l(i)$ using (15) 8. **end for** 9. Select path $P^l(i)$ with maximum $R^l(i)$ 10. **else** 11. Handover services of the unserved MSs to the neighbouring BSs or RSs 12. **end if** 13. **end for**

Fig. 13. Throughput based downlink path selection for MSs.

The stage-wise complexity analysis of the proposed scheme is illustrated in Table 3. The stage-wise computational complexity analysis of the proposed scheme is described as follows: In stage 1, the PP calculation in step 1 needs (M-1) additions and 1 multiplication. The average distance calculation in step 2 needs $5M+(M-1)$ additions, $3M+1$ multiplication and $2M$ access to a lookup table (LUT). The number of clusters formed in step 3 needs 1 addition. The initial MP calculation in steps 4 to 7 needs $4s$ addition, $8s$ multiplication and $2s$ access to LUT. The distance between every MP to all the MSs are identified between steps 8 to 13, which requires $5Ms$ addition, $3Ms$ multiplication and $2Ms$ LUT access. The final MP calculation in step 15 needs $s(U_j-1)$ additions and s multiplications. The steps 8 to 16 are iterated for q number of times. Thus, stage 1 requires $5Msq+4s+5M+2(M-1)+sq(U_j-1)+1$ additions, $3Msq+8s+3M+sq+2$ multiplications and $2M+2s+2Msq$ access to LUT respectively. In stage 2, for every cluster, the BS candidate location nearer to the final MP is identified between steps 2 to 5.

This computation needs $5b$ additions, $3b$ multiplications and $2b$ access to LUT. The T_c updated in step 6 needs 1 addition. The steps 1 to 7 needs $s(5b+1)$ additions, $3bs$ multiplications and $2bs$ access to LUT. The coverage ratio calculation in step 8 needs 1 multiplication. The average throughput obtained in step 9 requires $2(M-1)$ additions and $(M+1)$ multiplications. Thus, stage 2 totally requires $s(5b+1)+2(M-1)$ additions, $3bs+M+2$ multiplications and $2bs$ access to LUT respectively.In stage 3, step 2 needs $2s$ comparisons. The cell edge RS identification in step 4 requires $2rs$ additions and $2rs$ multiplication. The DF obtained between steps 7 to 9 needs $sr^j(M_{UMS}-1)$ additions, $3sr^j$ multiplications. The maximum DF identification in step 11 requires $s(r^j \ log \ r^j)$ comparisons. In step 14, T_c is updated, which needs sr^j additions. Step 19 requires 2 comparisons. Coverage ratio and average throughput update in step 24 requires $2(M-1)$ additions and $M+2$ multiplications. Thus, stage 3 requires $3sr+2(M-1)+sr^j(M_{UMS}-1)$ additions, $2sr+3sr^j+M+2$ multiplications and $2s+s(r^j \ log \ r^j)$ comparisons respectively. In stage 4, step 2 needs M_{CMS} comparisons. The steps 4 to 6 requires $M_{CMS} N_p(L^l-1)$ addition. Thus, stage 4 requires $M_{CMS}N_p(L^l-1)$ additions, M_{CMS} $(R^l \log R^l+1)$ comparisons.

The computational complexity of various MHR deployment schemes is compared in Table 4. The variable t used in a fuzzy logic based scheme represents the number of samples used to compute selection factor. In ACRD scheme, the variables T, F, C and w represents the number of tiers in the BS coverage range, the number of RS types, the number of deployment combinations and the number of parameter weights respectively. From Table 4, it is clear that the proposed scheme is computationally less complex than the conventional uniform clustering, ACRD schemes. Even though the fuzzy logic based scheme is less complex, our proposed scheme offers better performance in terms of coverage, throughput and power proportion.

Table 3. Stage-wise complexity analysis of the proposed scheme.

Stages	Number of additions	Number of multiplications	Number of comparisons	Number of access to LUT
1	$5Msq+4s+5M+2(M-1)+sq(U_j-1)+1$	$3Msq+8s+3M+sq+2$	-	$2M+2s+2Msq$
2	$s(5b+1)+2(M-1)$	$3bs+M+2$	-	$2bs$
3	$3sr+2(M-1)+sr^j(M_{UMS}-1)+sr^j$	$3sr^j+M+2+2sr$	$2s+s(r^j \ log \ r^j)+2$	-
4	$M_{CMS}N_p$ (L^l-1)	-	$M_{CMS}(R^l \log R^l+1)$	-

Table 4. Complexity comparison of various MHR deployment schemes.

Schemes	Number of additions	Number of multiplications	Number of comparisons	Number of access to LUT
Uniform clustering	13M-2+4s+sq(M-1)+ 5sb+br(M_{UMS}-1)+br(b+r-1)+(b+r)+2(b+r)(M-1)+ b(s-1)+b(b+r-1)+5r	8s+sq+3sb+3br+br(b+r)+ 2 (b+r) +b(b+r)+19M+14r+2	s(blogb)+br (rlogr)+br+2b+r	5M+2s+2sb +3r
Fuzzy	b(2t-1)+br(M_{UMS} -1)+ br(b+r-1)+2r(M-1)+ 6r+(b-1)+b(b+r-1)+6M	b(t+3)+3br+br (b+r)+b(b+r)+16r+16M+ 1	2b+br(r log r+1)	3(M+r)
ACRD	4T(F-1)+5(T-1)+ CTF+T(F+1)+4(w-1)+3C	5TF+3(T+1)+2T+CTF+C T (2F+2)+4C+17	3C	-
Proposed	5Msq+4s+5M+2(M-1)+sq(U_j-1)+1+ s(5b+1)+2(M-1)+3sr+2(M-1)+sr^j(M_{UMS}-1)+ sr^j +M_{CMS} N_p (L^l-1)	3Msq+8s+3M+sq+2+3bs +M+2+3sr^j+M+2+2sr	2s+s(r^j log r^i)+2+ M_{CMS} (R^l log R^l+ 1)	2M+2s+2M sq+2bs

4. Simulation Results and Discussion

In this section, the performance of the proposed scheme is tested with the simulation results. The parameters considered for the simulation study are listed in Table 5. The simulation is repeated for 100 different MS spatial distributions and the average values of the throughput and the coverage ratio are displayed in this work.

Table 5. Simulation parameters.

BS/RS settings	
Carrier frequency (GHz)	Taranetz et al. [42] 2.14
Placement cost (units)	Chang and Chen [33] BS: 9, RS: 3
Total power allocated (W)	Chang et al. [34] BS: 40, RS: 8
Coverage radius (km)	Chang and Lin [35] BS: 3.2, RS: 1.9
Interference threshold distance for RS (km)	Chang and Chen [33] and Chang and Lin [35] 0.5
Network layout settings	
Scenario	Wang and Chuang [43] Small group/Medium group/Large group
Size of the geographic area (km × km)	Wang and Chuang [43] 10×10 (small group) 15×15 (medium group) 20×20 (large group)
Network nodes	BS, RS and MS
Number of BS candidate locations	Chang and Chen [33] and Chang and Lin [35] 4-8
Number of RS candidate locations	Chang and Chen [33] and Chang and Lin [35] 4, 8, 12, 16, 20
Channel settings	
Large scale fading model	Chang and Chen [33], Chang et al. [34] and Chang and Lin [35] Free space propagation
Additive white Gaussian noise (AWGN) power (dBm/Hz)	Wang and Chuang [43] -174
MS settings	
MS density	Wang and Chuang [43] 300 to 500
Spatial distribution	Chang et al. [34] Non-homogeneous Poisson and uniform process
Downlink traffic demand (Mbps)	1 to 10
Other settings	
ECR	Chang and Chen [33] and Chang and Lin [35] 90%
***T* (Units)**	Wang and Chuang [43] 50 (Small group) 60 (Medium group) 80 (Large group)
$\overline{V_E}$ **(Mbps)**	5

The performance of the proposed scheme is validated for three scenarios namely small group, medium group and large group. The transmission power, cell radius and capacity from Table 1 are used for the simulation scenarios set up. Using these values, Figs. 14-17 are generated.

Similarly, Table 2 is used in average throughput per user (Mbps) measurements. Table 2 maps the distance between the nodes with the data rate. The algorithm identifies the nature of transmission (direct or indirect) for each covered user in the geographic area. Based on the transmission distance between the serving node and the user, the achievable data rates are calculated.

Assumptions [33, 35]:

- The candidate locations for BS and RS are randomly selected within the geographical area.
- The proposed scheme is tested only for downlink traffic demands.

The stage by stage execution of one of the sample small group simulation scenarios of the proposed scheme is shown in Figs. 14 to 17 respectively. During stage 1, PP and MPs are calculated. From Fig. 14, it is clear that two initial MPs are identified in the cluster formation stage to meet the throughput and the coverage requirements.

The steps 8 to 16 are iterated until all the MSs are fixed to a particular stage. The final MPs are also identified in the same stage. A sample simulation scenario for stage 2 is displayed in Fig 15. The proposed scheme identifies the BS candidate locations nearer to the identified final MPs.

Two macro BSs are placed during stage 2. After deploying BSs, the obtained coverage and average throughput per user values are compared with the expected requirements. If the requirements are not met, the deployment of RSs is carried out in stage 3. A sample simulation scenario for stage 3 is displayed in Fig. 16.

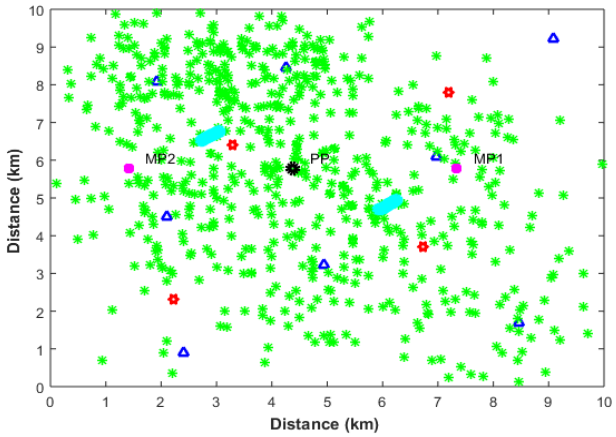

Fig. 14. Sample small group scenario for stage 1.

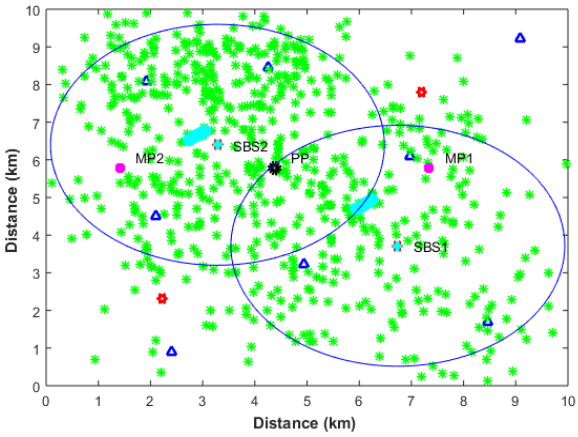

Fig. 15. Sample small group scenario for stage 2.

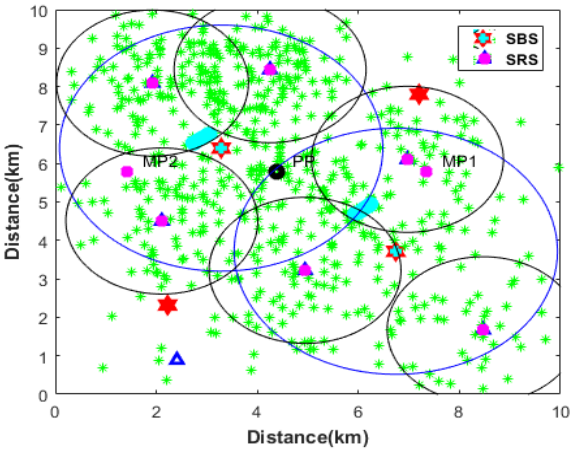

Fig. 16. Sample small group scenario for stage 3.

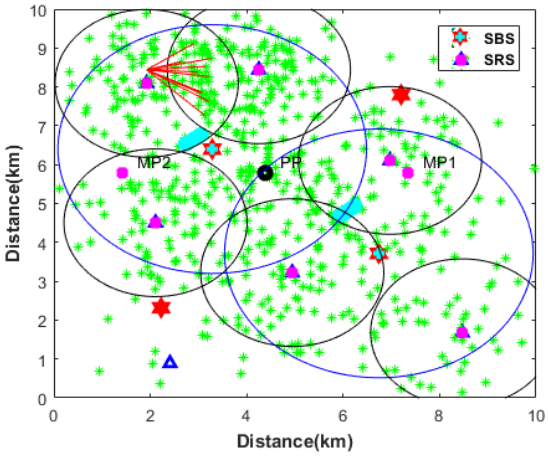

Fig. 17. Sample small group scenario for stage 4.

To meet the requirements, six RS candidate locations are selected out of eight. It is also clear that the proposed scheme gives priority for the RS candidate locations in the cell edge. For the considered simulation scenario, our proposed scheme attains a coverage of more than 95%. The total deployment cost is 36 units, which is less than the total deployment budget. A sample simulation scenario for stage 4 is displayed in Fig. 17. The radio resource availability check and link traffic overloading conditions are checked in stage 4. Some of the MSs in the overlapping area is handed over to the neighbouring SRS. This is highlighted with red colour lines.

To meet the requirements, six RS candidate locations are selected out of eight. It is also clear that the proposed scheme gives priority for the RS candidate locations in the cell edge. For the considered simulation scenario, our proposed scheme attains a coverage of more than 95%. The total deployment cost is 36 units, which is less than the total deployment budget. A sample simulation scenario for stage 4 is displayed in Fig. 17. The radio resource availability check and link traffic overloading conditions are checked in stage 4. Some of the MSs in the overlapping area is handed over to the neighbouring SRS. This is highlighted with red colour lines.

For small group scenario, the average throughput per user achieved is compared between five different deployment schemes and results obtained are displayed in Fig. 18. It is clear that the increase in the number of candidate locations of the RS will also increase the system throughput initially. However, after a certain number of RSs, the throughput remains almost the same due to the co-channel interference and other issues. For twenty candidate positions of RSs, JBRP scheme offers an average system throughput of 7.2 Mbps. Similarly, ACRD, uniform clustering, fuzzy logic based schemes offer an average throughput of 8.3, 8.8 and 9.2 Mbps respectively. Our proposed scheme offers an average throughput of 9.5 Mbps, which is almost double than the expected. Our proposed scheme offers 2.55% and 6.78% improvement over the conventional fuzzy logic and uniform clustering based schemes in terms of throughput. This increment is mainly due to the inclusion of throughput-oriented selection rule, radio resource availability check and the robustness of the proposed algorithm under link traffic overloading conditions.

For small group scenario, the average coverage ratio achieved is compared between five different deployment schemes and results obtained are displayed in Fig. 19. It is clear that the increase in the number of candidate positions of RS increases the coverage ratio. For twenty candidate positions of RSs, JBRP scheme offers a coverage ratio of 79.12%, which is below the expected. Similarly, ACRD uniform clustering, fuzzy logic based schemes offer an average coverage ratio of 84.82%, 88.48% and 89.12% respectively. Our proposed scheme offers an average coverage ratio of 94.11%, which is above the expected. Our proposed scheme offers 5.3% and 5.98% improvement over the conventional fuzzy logic and uniform clustering based schemes in terms of service coverage. Since our proposed scheme motivates RS deployment in the cell edges, it can cover number of MSs than the other conventional schemes. The LASER based service handover also increases the connection density. It is also noted that the average deployment budget of the proposed scheme is 36 units, which is less than the actual allocated deployment budget. Thus, the proposed scheme reduces the cost per bit than the other conventional schemes.

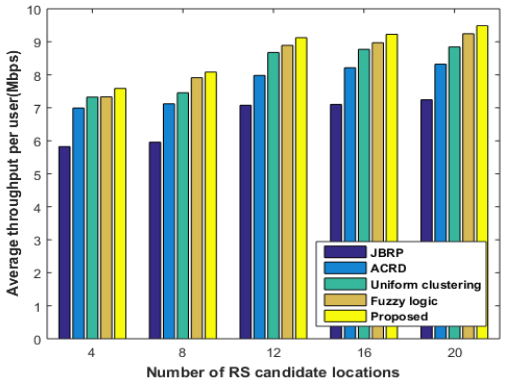

Fig. 18. Average throughput per user (Mbps) comparison of small group scenario for different deployment schemes.

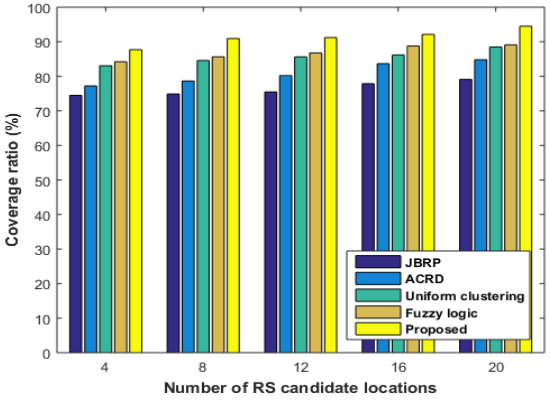

Fig. 19. Coverage ratio (%) comparison of small group scenario for different deployment schemes.

The sample stage 4 of medium and large group scenarios are displayed in Figs. 20 and 21 respectively. It is also noted that the average deployment cost of the proposed scheme for medium and large group scenarios are 48 and 66 units respectively, which are less than the allocated deployment budget. Hence, it is proved that the proposed scheme minimizes the cost per bit for different network sizes. The average throughput per user performance is compared between five different deployment schemes for three different network sizes and the results obtained are displayed in Fig. 22. The number of RS candidate sites is fixed to be 20. It is clear that the proposed scheme achieves improved throughput than the conventional schemes for all the three network sizes.

The average coverage ratio performance is compared between five different deployment schemes for three different network sizes and the results obtained are displayed in Fig. 23. The number of RS candidate sites is fixed to be 20. It is clear that the proposed scheme achieves improved coverage ratio than the conventional schemes for all the three network sizes. The required coverage ratio of 90% is achieved for all the network sizes. The proposed algorithm prioritizes the RSs at the cell edges. This feature increases the coverage ratio.

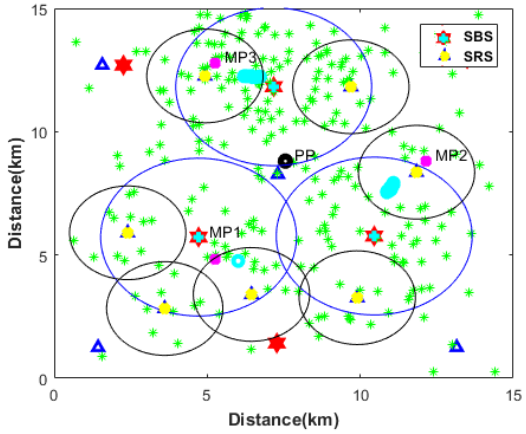

Fig. 20. Sample medium group scenario for stage 4.

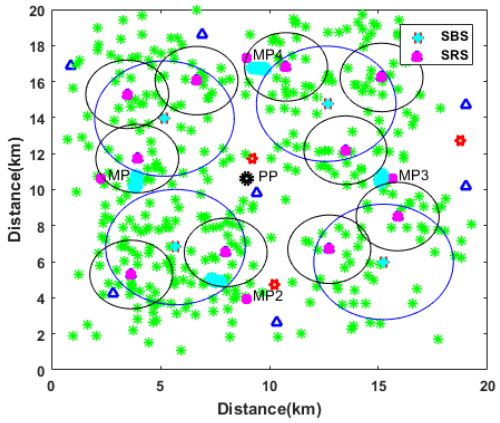

Fig. 21. Sample large group scenario for stage 4.

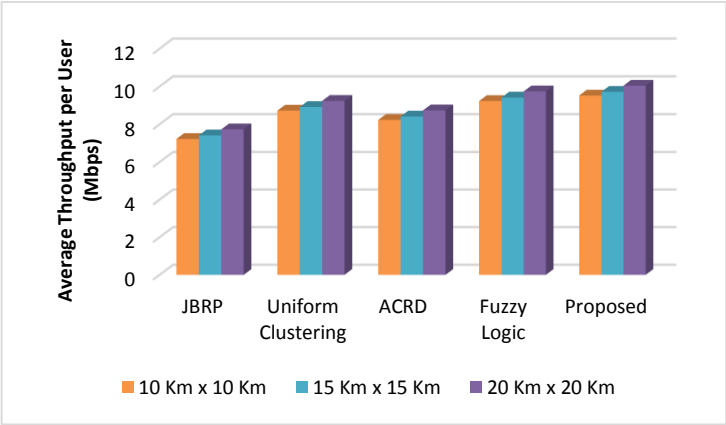

Fig. 22. Average throughput per user (Mbps) comparison between various deployment schemes for different network sizes.

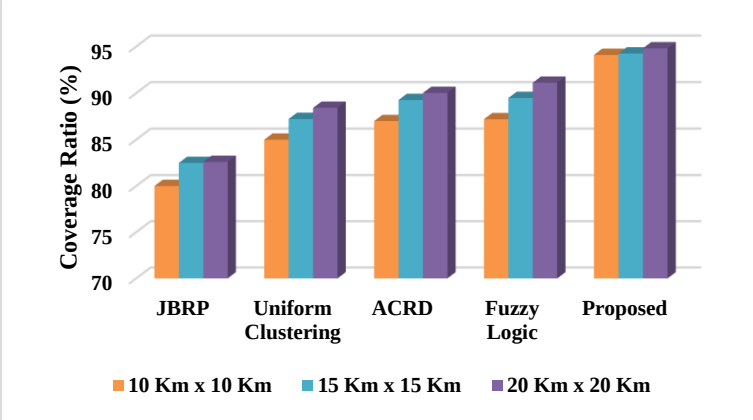

Fig. 23. Coverage ratio (%) comparison between various deployment schemes for different network sizes.

5. Conclusions

Through simulation results, it is observed that the proposed scheme outperforms the traditional JBRP, ACRD, uniform clustering and fuzzy logic based schemes in terms of coverage, cost, and throughput. The results are also validated for various network sizes. Due to the inclusion of throughput-oriented selection rule, our proposed scheme outperforms all the other considered schemes even under link overloading conditions. Thus, it can be considered as one of the promising candidates for next-generation networks to maximize per user throughput and to minimize the cost per bit.

The promising results pave a path for the further investigation of the proposed scheme under co-channel interference and shadowing environments. As of now, the network operators have deployed numerous macro BSs. Since site procurement is costly, it is extremely hard to redeploy new macro BSs. Hence, the proposed scheme can be adjusted in a manner that it can utilize the current deployed macro BSs and adds RSs to fulfil the traffic demands of the clients in a cost-effective way.

Nomenclatures

B^c	Set of BS candidate positions
b	Number of candidate positions of BS
C_i^{BS}	Deployment cost of ith BS
C_i^{RS}	Deployment cost of ith RS
d_I	Interference threshold distance
$L^l(i)$	Length of the l^{th} path of a i^{th} MS
M	Total number of MSs in the geographic area
M_{CMS}	Number of covered MSs
MP	Coordinates of final mean point
M_{UMS}	Number of uncovered MSs
m_{jx}, m_{jy}	Coordinates of initial MP

$N_p(i)$	Number of possible downlink paths of a i^{th} MS
R	Data transmission rate of a user
R_{BS}	Radius of BS
R_{bm}	Data transmission rate between BS and MS
R_{brm}	Data transmission rate between BS, RS and MS
R^c	Set of RS candidate position
$R^l(i)$	Total transmission rate of l^{th} path of i^{th} MS
R_i^{MS}	Transmission rate between BS and i^{th} MS
r	Number of candidate positions of RS
s	Number of clusters formed
T_c	Total deployment cost
U_j	Number of MSs joined to the j^{th} cluster
T	Total deployment budget
$\bar{V}$	Average throughput per user
$\overline{V_E}$	Expected average throughput
Z_i	Coordinates of MSs

Greek Symbols

α_i	Binary variable of MS
β_i γ_i	Binary variable of BS and RS

Abbreviations

BS	Base Station
CR	Coverage Ratio
ECR	Expected Coverage Ratio
LASER	Load-Aware Spectral Efficient Routing
MHR	Multi-Hop Relay
MS	Mobile Station
RS	Relay Station
SBS	Selected BS Locations
SRS	Selected RS Locations

References

1. Aguero, R.; Choque, J.; Irastorza, J.A.; and Munoz, L. (2011). Coverage extension by means of non-conventional multi-hop communications. *Computer Communications*, 34(18), 2195-2206.
2. Bilbao, M.N.; Del Ser, J.; Perfecto, C.; Salcedo-Sanz, S.; and Portilla-Figueras, J.A. (2018). Cost-efficient deployment of multi-hop wireless networks over disaster areas using multi-objective meta-heuristics. *Neurocomputing*, 271, 18-27.
3. IEEE. (2011). P802.11s – IEEE Draft standard for information technology, telecommunications and information exchange between systems, local and metropolitan area networks, specific requirements. Part 11: Wireless LAN medium access control (MAC) and physical layer (PHY) specifications, amendment 10: Mesh networking.

4. IEEE Standard Association. (2009). IEEE 802.16j-2009 – IEEE standard for local and metropolitan area networks, Part 16: Air interface for broadband wireless access systems amendment 1: Multihop relay specification. Broadband Wireless Access Working Group
5. Schoenen, R.; Halfmann, R.; and Walke, B.H. (2008). MAC performance of a 3GPP-LTE multihop cellular network. *Proceedings of the IEEE International Conference on Communications (ICC)*. Beijing, China, 4819-4824.
6. Beniero, T.; Redana, S.; Hamalainen, J.; and Raaf, B. (2009). Effect of relaying on coverage in 3GPP LTE-advanced. *Proceedings of the IEEE 69th Vehicular Technology Conference (VTC Spring)*. Barcelona, Spain, 1-5.
7. Irmer, R.; and Diehm, F. (2008). On coverage and capacity of relaying in LTE-advanced in example deployments. *Proceedings of the 19th IEEE International Symposium on Personal, Indoor and Mobile Radio Communications*. Cannes, France, 1-5.
8. Kocan, E.; Domazetovic, B.; and Pejanovic-Djurisic, M. (2017). Range extension in IEEE 802.11ah systems through relaying. *Wireless Personal Communications*, 97(2), 1889-1910.
9. Pabst, R.; Walke, B.H.; Schultz, D.C.; Herhold, P.; Yanikomeroglu, H.; Mukherjee, S.; Viswanath, S.; Lot, M.; Zirwas, W.; Dohler, M.; Aghwami, H.; Falconer, D.D.; and Fettweis, G.P. (2004). Relay-based deployment concepts for wireless and mobile broadband radio. *IEEE Communications Magazine*, 42(9), 80-89.
10. Rehman, O.; Ould-Khaoua, M.; and Bourdoucen, H. (2016). An adaptive relay nodes selection scheme for multi-hop broadcast in VANETs. *Computer Communications*, 87, 76-90.
11. Lai, C.-C.; Lee, R.-G.; Hsiao, C.-C.; Liu, H.-S.; and Chen, C.-C. (2009). A H-QoS-demand personalized home physiological monitoring system over a wireless multi-hop relay network for mobile home healthcare applications. *Journal of Network and Computer Applications*, 32(6), 1229-1241.
12. Yuan, B.; Chen, H.; and Yao, X. (2017). Optimal relay placement for lifetime maximization in wireless underground sensor networks. *Information Sciences*, 418-419, 463-479.
13. Dao, N.-N.; Park, M.; Kim, J.; Paek, J.; and Cho, S. (2018). Resource-aware relay selection for inter-cell interference avoidance in 5G heterogeneous network for internet of things systems. *Future Generation Computer Systems*, 93, 877-887.
14. Arthi, M.; Arulmozhivarman, P.; and Babu, K.V. (2015). Quality of service aware multi-hop relay networks for green radio communication. *Journal of Green Engineering*, 5(2), 1-21.
15. Arthi, M.; Arulmozhivarman, P.; and Babu, K.V. (2016). A quality-aware relay station deployment scheme for green radio communication. *Journal of Green Engineering*, 6(2), 1-27.
16. Chen, H.; Chen, W.; and Zhao, F. (2016). Energy-efficient mobile relay deployment scheme for cellular relay networks. *Ad Hoc Networks*, 51, 36-46.
17. Suarez, L.; Nuaymi, L.; and Bonnin, J.-M. (2012). An overview and classification of research approaches in green wireless networks. *EURASIP Journal on Wireless Communications and Networking*, 142, 18 pages.

18. Arthi, M.; and Arulmozhivarman, P. (2017). Power-aware fuzzy based joint base station and relay station deployment scheme for green radio communication. *Sustainable Computing: Informatics and Systems*, 13, 1-14.
19. Murugadass, A.; and Pachiyappan, A. (2017). Fuzzy logic based coverage and cost effective placement of serving nodes for 4G and beyond cellular networks. *Wireless Communications and Mobile Computing*, Article ID 8086204, 25 pages.
20. Arthi, M.; and Arulmozhivarman, P. (2016). A flexible and cost-effective heterogeneous network deployment scheme for beyond 4G. *Arabian Journal for Science and Engineering*, 41(12), 5093-5109.
21. Ullah, I.; Mutafungwa, E.; Hämäläinen, J.; and González, D.G. (2018). A simple approach for the suppression of Rician interference in a relay backhaul using limited feedback. *Physical Communication*, 29, 171-182.
22. 3GPP. (2017). 3rd generation partnership project, technical specification group radio access network; Evolved universal terrestrial radio access (E-UTRA), Physical channels and modulation (Release 13).
23. Loa, K.; Wu, C.-c.; Sheu, S.-t.; Yuan, Y.; Chion, M.; Huo, D.; and Xu, L. (2010). IMT-advanced relay standards [WiMAX/LTE update]. *IEEE Communications Magazine*, 48(8), 40-48.
24. Salem, M.; Adinoyi, A.; Rahman, M.; Yanikomeroglu, H.; Falconer, D.; Kim, Y.-D.; Kim, E.; and Cheong, Y.C. (2010). An overview of radio resource management in relay-enhanced OFDMA-based networks. *IEEE Communications Surveys and Tutorials*, 12(3), 422-438.
25. Saleh, A.B.; Redana, S.; Hamalainen, J.; and Raaf, B. (2010). On the coverage extension and capacity enhancement of inband relay deployments in LTE-advanced networks. *Journal of Electrical and Computer Engineering*, Article ID 894846, 12 pages.
26. Hoymann, C.; Chen, W.; Montojo, J.; Golitschek, A.; Koutsimanis, C.; and Shen, X. (2012). Relaying operation in 3GPP LTE: challenges and solutions. *IEEE Communications Magazine*, 50(2), 156-162.
27. Cheng, M.X.; Ling, Y.; and Sadler, B.M. (2017). Network connectivity assessment and improvement through relay node deployment. *Theoretical Computer Science*, 660, 86-101.
28. Senel, F.; and Younis, M. (2016). Novel relay node placement algorithms for establishing connected topologies. *Journal of Network and Computer Applications*, 70, 114-130.
29. Lu, H.-C.; and Liao, W. (2009). Joint base station and relay station placement for IEEE 802.16j networks. *Proceedings of IEEE Global Telecommunications Conference (GLOBECOM)*. Honolulu, Hawaii, USA, 1-5.
30. Tutschku, K. (1998). Demand-based radio network planning of cellular mobile communication systems. *Proceedings of Seventeenth Annual Joint Conference of the IEEE Computer and Communications Societies (INFOCOM'98)*. San Francisco, California, United States of America, 1054-1061.
31. Zhang, W.; Bai, S.; Xue, G.; Tang, J.; and Wang, C. (2011). Darp: Distance-aware relay placement in wimax mesh networks. *Proceedings of IEEE INFOCOM*. Shanghai, China, 2060-2068.

32. Wu, G.; and Feng, G. (2012). Energy-efficient relay deployment in next generation cellular networks. *Proceedings of IEEE International Conference on Communications (ICC)*. Ottawa, Canada, 5757-5761.
33. Chang, J.-Y.; and Chen, Y.-W. (2015). A cluster-based relay station deployment scheme for multi-hop relay networks. *Journal of Communications and Networks*, 17(1), 84-92.
34. Chang, B.-J.; Liang, Y.-H.; and Su, S.-S. (2015). Analyses of relay nodes deployment in 4G wireless mobile multihop relay networks. *Wireless Personal Communications*, 83(2), 1159-1181.
35. Chang, J.-Y.; and Lin, Y.-S. (2015). An efficient base station and relay station placement scheme for multi-hop relay networks. *Wireless Personal Communications*, 82(3), 1907-1929.
36. Wang, S.-S.; Lien, C.-Y.; Liao, W.-H.; and Shih, K.-P. (2012). LASER: A load-aware spectral-efficient routing metric for path selection in IEEE 802.16j multi-hop relay networks. *Computers and Electrical Engineering*, 38(4), 953-962.
37. Li, X.; Guo, D.; Grosspietsch, J.; Yin, H.; and Wei, G. (2016). Maximizing mobile coverage via optimal deployment of base stations and relays. *IEEE Transactions on Vehicular Technology*, 65(7), 5060-5072.
38. Liao, Z.; Liang, J.; and Feng, C. (2017). Mobile relay deployment in multihop relay networks. *Computer Communications*, 112(C), 14-21.
39. Magan-Carrion, R.; Rodriguez-Gomez, R.A.; Camacho, J.; and Garcia-Teodoro, P. (2016). Optimal relay placement in multi-hop wireless networks. *Ad Hoc Networks*, 46, 23-36.
40. Wang, S.-S.; Yin, H.-C.; Tsai, Y.-H.; and Sheu, S.-T. (2007). An effective path selection metric for IEEE 802.16-based multi-hop relay networks. *Proceedings of the IEEE Symposium on Computers and Communications.* Las Vegas, Nevada, United States of America, 1051-1056.
41. Swain, C.M.K.; and Das, S. (2018). Effects of threshold based relay selection algorithms on the performance of an IEEE 802.16j mobile multi-hop relay (MMR) WiMAX network. *Digital Communications and Networks*, 4(1), 58-68.
42. Taranetz, M.; Blazek, T.; Kropfreiter, T.; Müller, M.K.; Schwarz, S.; and Rupp, M. (2015). Runtime precoding: Enabling multipoint transmission in LTE-advanced system-level simulations. *IEEE Access*, 3, 725-736.
43. Wang, Y.-C.; and Chuang, C.-A. (2015). Efficient eNB deployment strategy for heterogeneous cells in 4G LTE systems. *Computer Networks*, 79, 297-312.